"Enhancing Brain Tumor Classification through a Hybrid Feature Extraction Approach with Regularized Extreme Learning Machine"

Mr. Sarvesh Warjurkar1, Dr. Sonali Ridhorkar2

1 Research Scholar(Ph.D), Department of CSE, GHRU, Amravati, MS, India
2 Associate Professor, GHRIET, Nagpur, MS, India
Email:- sarveshphd3690@gmail.com, sonaliridhorkar@gmail.com

ABSTRACT:

The classification of brain cancer is the crucial process that vigorously depends on the knowledge and experience of physicians. To aid radiologists and doctors in identifying brain tumors, it is crucial to have a computerized framework for the classification of tumor. Be that as it may, the exactness of current frameworks needs enhancement to ensure appropriate treatment. In this research paper, we suggest an accurate classification of brain tumor approach by combining a blend component uprooting strategy with a Regularized Extreme Learning Machine (RELM). The point of view includes pre-handling brain images utilizing a standardization rule of min-max to upgrade the difference of brain regions and edges. Subsequently, the traits of tumors are uprooted by using a blend component extraction strategy. At the end, the RELM algorithm is employed to classify the brain tumor type. To access and analyze the suggested strategy, a series of investigations is performed using a brain image dataset. The investigation outputs demonstrate that, a methodology is higher viable than existing cutting-edge methods. The classification accuracy, measured using the random holdout technique, improved from 91.57% to 94.43% with the proposed approach.

Keywords: Hybrid feature extraction, classification of brain tumors, RELM, N G I S T- P C A.

I.   INTRODUCTION:

Through a large number of connections and neurons, the brain is the body's primary control centre, facilitating a wide range of activities. Brain cancers, strange cell developments inside the brain, represent a huge danger to the working of the nervous system. These growths can be either harmful (dangerous) or harmless (non-destructive). Early discovery of brain tumors is vital for fruitful treatment, depending on the information and ability of doctors [2]. When it comes to assisting doctors in making informed treatment decisions, a computerized classification system of brain tumor is an extremely useful mechanism. Magnetic resonance (MR) imaging devices, which are widely used by radiologists to diagnose the brain, serve as the basis for these systems [1]. In last few years, various research studies and automated systems were developed to classify and detect brain tumors by having the use of MRI. For example, Sompong and Wongthanavasu [4] suggested a hybrid system utilizing the c-means fuzzy algorithm for the segmentation of brain tumors. They tended to the seed-developing issue by presenting another likeness capability with a grey level co-event framework (GLCM), assessing their strategy on the BraTS2013 dataset. Sehgal et al. [3] presented an computerized technique for the purpose of finding brain tumors by using the tumor extraction and image segmentation methods. They employed circularity and area features to extract tumors from segmented brain images, achieving an average similarity of 0.729 (72.9%) when compared to ground truth images. In [6], by initiating an active contour model and creating a feature map from MR images using human interaction to divide the region of interest (ROI), a semi-computerized method for the segmentation of MRI brain image was developed. Examination with ground truth return for capital invested pictures, physically divided from the first pictures, was performed utilizing cross-over record boundary and Jaccard coefficient. G. B. Praveen and A. Agrawal

[5] proposed a method with multiple stages for brain cancer discovery from MRI, including picture pre-handling (editing, noise reducing, histogram levelling and scaling), extraction of features (histogram techniques and GLCM), and order utilizing an random forest (RF) classifier. The methodology was tried on a huge dataset of 124 patients, achieving a classification accuracy of 87.62%. Another study [8] utilized wavelet-based feature extraction from MRI's, employing a Markov Random Field model (M R F) for image segmentation. In their research, Abbasi and Tajeripour [7] introduced a computerized approach for the purpose of finding brain tumors within 3D images. Their methodology entails the segmentation of the Region of Interest (ROI) from background, achieved through histogram matching and bias field correction. The Random Forest (RF) algorithm is used to detect brain tumors following this pre-processing. Evaluations were performed on the B R A T S 2013 data-set. Various techniques of deep learning, including the utilization of multiple Convolutional Neural Networks (CNNs) coupled with methods of discrimination [9]-[10], as well as the adoption of a single CNN approach [11], have been introduced as viable approaches for the classification of brain tumors in CT images. In [12],[13] and [14],researchers presented an architecture for the classification of brain tumors, utilizing convolution and pooling operations to extract attributesfrom the given input brain images. Ari and Hanbay [16] put forth a deep learning approach employing Extreme Learning Machine with Local Receptive Fields (E L M-L R F) to distinguish between malignant and benign brain tumors. Their evaluation was carried out on a 16 patient images make up this data set, with 09 utilized for training and 07 for testing. It's worth noting that while deep learning techniques enhance tumor classification, they demand a substantial volume of training data, significant computational resources, and extended training durations [16].

The R E L M is a method of classification and regression that has gained popularity in various applications, mainly due to its ability to address certain drawbacks associated with the back-propagation method [17]. The RELM offers advantages such as faster training speed and lower complexity compared to other classifiers.

This work introduces several key contributions outlined as follows:

An automatic approach is suggested for the classification of brain tumor, aiming to assist doctors and radiologists in identifying the sort of brain-cancer.

An innovative and efficient hybrid feature extraction technique, known as PCA-NGIST, is presented. This approach merges the Normalized GIST descriptor with Principal Component Analysis (PCA) to capture important characteristics from brain images, all while avoiding the need for image segmentation. This is particularly crucial because segmentation methods can be vulnerable to variations in lighting and shading, which can lead to imprecise outcomes when classifying brain tumors.

The R E L M classifier is utilized in this approach due to the property of regularization, this aid in mitigating the problem of overfitting, and it also boasts rapid training speed. The parameters of the suggested method are fine-tuned through a grid search algorithm, guaranteeing the attainment of optimal performance. The suggested method is assessed using a newly available dataset of public brain images and is then benchmarked against the most recent techniques comparing the same dataset is utilising.

The remaining information in the document is arranged as follows: The suggested technique is described in depth in Section II, experiments and debates are covered in Section III, and the study's overall conclusion is presented in Section IV.

II. PROPOSED APPROACH

We give a thorough review of in this section of our proposed methodology, which consists of three primary steps: (i) The preprocessing of brain image, (ii) Feature extraction of Brain and (iii)

Classification of Brain Tumors. The input for this method consists of MRI brain images, and the outcome is the corresponding categorization of the brain tumor. Figure:1 illustrates a flow of our suggested way. The following subsections describe specifics of each step in detail.

i).   Pre-processing of Brain Image

The quality of brain feature extraction as well as the outcomes of brain image analysis are both significantly influenced by the pre-processing of brain images, which is a crucial step. Often, while interpreting input MRIs, they may contain values that exceed the [0, 255] range, and they might even include non positive values. Consequently, in our method, the transformation of the brain image into intensity-based representations is the main goal of this step within the [0, 1] extent. To accomplish this transformation, we employ a min—max rule of normalization, as illustrated by the following equation:

$$f(x, y) = \frac{f(x, y) - V_{min}}{V_{max} - V_{min}}$$ .....(1)

where min(f) and max(f) are the picture's lowest and highest values, and f(x, y) represents each pixel in the brain image, respectively. In this equation, Original image constitutes the values of pixels of the brain images, "min value" refers to the minimum pixel value present within the image, while the "max value" denotes the maximum pixel value within the image. By applying this normalization, the intensity of the brain images is rescaled to the range [0, 1], allowing for consistent and standardized processing in subsequent steps of the approach. By utilizing this technique, we enhance and improve the difference between brain areas and edges. This means that, boundaries and distinct qualities within the brain image become more pronounced and easier to perceive. To visualize the effect, Figure-2 demonstrates an instance that showcases the source image before the contrast enhancement step and the corresponding output image after the enhancement process

ii) Feature Extraction of Brain

- G I S T Descriptor

A feature descriptor is G I S T originally introduced by Torralba and Olive for classification of image. It characterizes image features according to the spatial envelope, which represents the image in two dimensions. By combining different scales and orientations of Gabor filters with the image, the GIST aspects are able to capture an image's notable spatial structure. This convolution process generates a set of filtered images, each having the same size as the input image. These filtered images are then divided into a grid structure. Within each grid cell, the average value is computed. Subsequently, the average values from all the grid cells are concatenated, resulting in a set of GIST feature vectors. The total number of GIST feature vectors depending on how many grid cells and how many filtered images produced by Gabor Filters.
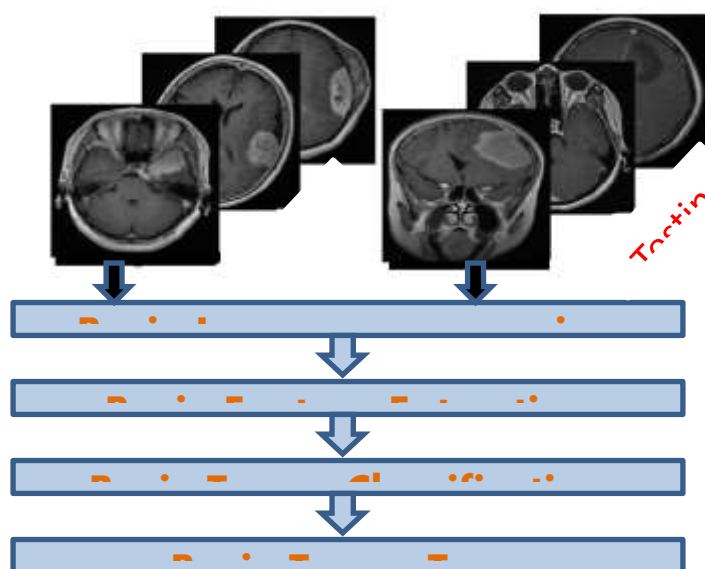
Figure-1: Proposed approach Flowchart

<center>(i)   (ii)</center>
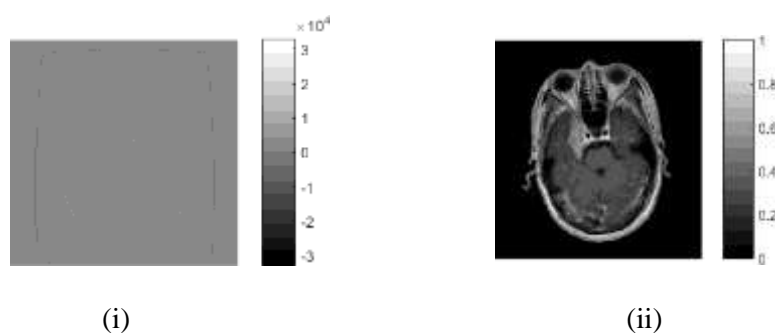
Figure-2: The input and output of the pre-processing phase of an image

(i) Raw data values of the input image of brain   (ii) outcome of image displaying intensity values of brain data

- Fusion of Different Elements P C A - N G I S T Method

The fusion technique known as P C A - N G I S T is a method used to extract features. It combines Principal Component Analysis (P C A) with the normalized G I S T (N G I S T) descriptor. N G I S T is an updated version of the traditional G I S T descriptor, originally submitted by Gumaei et al. The N G I S T descriptor addresses issues such as varying illumination and shadows in images by normalizing them through the L2 norm.

The NGIST descriptor presents images in a compact, low-dimensional format, summarizing their orientations and scales. It offers a broad overview of normalized features without the need for image segmentation. In contrast, P C A is a commonly employed technique for reducing dimensionality and extracting features. The goal is to create a condensed set of significant highlights got from the first Essence highlights. This is done to minimize the risk of overfitting during the arrangement stage.s

In the P C A- N G I S T approach, G I S T features are computed based on brain images. The eigenvectors linked to the most significant eigen values are then determined from these features. These eigenvectors capture the most vital information within the data. Following this, the GIST features are projected onto a fresh feature subspace, which has an equal or reduced number of dimensions, using the chosen eigenvectors. This process aids in reducing the feature space's dimensionality while preserving the most distinctive information for classification purposes.

Let's imagine, "f (x, y)" represents a 2-Dimentional Gabor filter applied to an image of the brain across "n" orientations and "m". This filter is calculated as follows:

$$f(x, y) = \left(\frac{1}{2\pi\sigma_x\sigma_y}\right)\exp\left[-\frac{1}{2}\left(\frac{x^2}{\sigma_x^2} + \frac{y^2}{\sigma_y^2}\right) + 2\pi j\omega x\right] \quad\quad .....(2)$$

In this context ω indicates the Gabor filter's Radial Frequency (RF), 'j' represents a perplexing number equal to $\sqrt{-1}$ and σ_x and σ_y are components of the Gabor filter's overall and asymmetrical foundation [20]. By having the use of 2-Dimentional Gabor filter having capability "f(x, y)," the Fourier Transform Function "F(u, v)" can be denoted as follows:

$$F(u,v) = \exp\left\{-\frac{1}{2}\left[\frac{(u-\omega)^2}{\sigma_u^2} + \frac{v^2}{\sigma_v^2}\right]\right\} \quad\quad .....(3)$$

Where σ_u and σ_v are calculated as:

$$\sigma_u = \frac{1}{2}\pi\sigma_x \quad \text{and} \quad \sigma_v = \frac{1}{2}\pi\sigma_y \quad\quad .....(4)$$

The Gabor wavelet transform uses a mother function represented by f(x, y). The Gabor Filter dictionary has been formed by configuring the parameters of orientation (θ) and scaling factor (δ). The orientation parameter determines the direction of the filter's receptive field, while the scaling factor controls the size of the receptive field.

$$f_{mn}(x, y) = \delta^{-m}f(x', y') \quad\quad .....(5)$$

At which $\delta > 1$, "n" and "m" are the integers denoting orientation and scale numbers, respectively. $\theta = n\pi/N$ And x' and y' is calculated here as follows:

$$x' = \delta^{-m}(x\cos\theta + y\sin\theta) \quad\quad .....(6)$$

$$y' = \delta^{-m}(-x\sin\theta + y\cos\theta) \quad\quad .....(7)$$

In this scenario, O represents the orientation number. The value of θ is computed as follows: $\theta = \theta = \frac{n\pi}{O}$. The parameter of scale δ^{-m} in equations (4,5 and 6) are choices to increase energy independence [20].

During the brain feature extraction process, Gabor filters are utilized on brain images with four unmistakable scales and eight unique orientations. This results in a combination of 32 filtered brain images. These filtered images are then divided into blocks. The number and size of these blocks are not explicitly mentioned. To generate a GIST feature vector, the value of average intensity within every block is figured. This process is applied to all the blocks in the filtered images, resulting in a GIST Feature Vector (G) with a combination of 512 features. This is based on the assumption that the blocks are evenly distributed across the filtered images. To obtain the normalized GIST (NGIST), the individual feature vectors (Gi) are normalized using the L2 norm. Normalizing the feature vectors based

on the L2 norm helps address issues related to transformation in illumination & shadowing. The specific normalization process is not described in the provided text

$$G_i = \frac{G_i}{\sqrt{\sum_{j=1}^{512} G_i^{\,2}}}$$

.....(8)

Let's assume that matrix T comprises a collection of NGIST brain characteristic vectors (Gi). To alleviate redundancy within these feature vectors, an unsupervised learning algorithm, namely Principal Component Analysis (PCA), is employed. PCA is used to calculate a matrix of chosen eigenvectors *(EV512xK),* where K represents the number of selected eigenvectors. Later on, these eigenvectors will be utilized to transform the matrix *TN X 512* into a more condensed characteristic matrix, $Y_{N \times K}$ by accompanying condition [21]:

$$Y_{N \times K} = T_{N \times 512} . EV_{512 \times K}$$ .....(9)

An algorithm process of P C A for calculating a matrix EV512 X K can be outlined as follows: We consider L as the count of mind growth classes inside the preparation data-set (T), consisting of N G I S T vectors: fG1, G2, G3, G4,......, GN, in which each Gi is a Real Number. Every training vector is associated with a class j from a set {1, 2, 3, 4, ... , L}. The lattice of covariance is characterized as follows :

$$S = \frac{1}{N-1} \sum_{i=1}^{N} (G_i - \overline{G}).(G_i - \overline{G})^T$$ .....(10)

In which G represents the vectors' average over all training data, and it's computed follows:

$$\overline{G} = \frac{1}{N} \sum_{i=1}^{N} G_i$$ ....(11)

The selection of K eigen vectors ($EV_{512 \times K}$)can be performed from the initial matrix of eigenvectors ($EV_{512 \times 512}$)correspond to the top K eigen values obtained through the covariance matrix's (S) decomposition, which is shown in the following manner:

$$EV_{512 \times K} = EV(i, j)$$ .....(12)   where 'i' = 1,2,3,4,.....,512 and 'j' = 1,2,3,4,.....,K.

iii) Classification of Brain Tumors

The last stage of proposed strategy involves the brain tumor classification, where the type of tumor is identified by having the use of RELM classifier. RELM stands for randomized ectreme learning machine, which is a kind of a neural network that feeds forward (FNN). It includes a single secret layer, a result layer, and an information layer. In instatement stage, the info layer's loads and predispositions are picked haphazardly. The weights for the output layer are then calculated. The RELM classifier employs the principles of Extreme Learning Machines (ELM) for multiclass classification, a concept suggested by Huang et al. in their research. At this point in the training process, the R E L M model for classification is constructed using the characteristics of brain got from preceding stage, which are assumed to be the normalized GIST features. The model is taught to recognize the distinct patterns and traits linked to various brain tumor types. After the model is trained, it can proficiently categorize the brain tumor type. Algorithm 1 seemingly delineates the inputs and outputs of this classification stage, providing an overview of the specific actions and procedures used when applying the trained RELM classifier for brain tumor classification. Regrettably, without access to the algorithm, we're unable to offer an intricate explanation of its particular implementation and functionality.

III. EXPERIMENTS AND DISCUSSIONS

A) Dataset

Datasets from Cheng [25, 26] were used in this exploration. It carries 3066 Magnetic resonance imaging (MRI) scans of brain tumors. Transverse, lateral, and frontal planes were used to capture the pictures from 233 patients. 996 axial pictures, 1024 sagittal images, and 1046 coronal images were divided into three groups. The collection includes photos of meningioma (1424 images), glioma (707 images), and pituitary (931 images), three different forms of brain tumours. The original dimensions of each image were 512 by 512 pixels. The creator of this dataset arranged the tumour mask pictures, tumour boundary coordinates, patient ID, labels, and brain images in the MATLAB data form. Samples of photos from a collection is displayed in the figure 3.

Brain tumour classification algorithm 1

The input consists of parameters, a testing and training dataset containing the features of brain after extraction, and training labels.

Testing labels (lj)

1. The training stage.

1.1. Initialising the biases and weights

1.1.1. Randomly picking the inputs biases(bi) along with weights (wi) for a RELM input layer

1.2. Calculation of Matrix

1.2.1. Using Eq. (13), Compute the hidden matrix layer (H) as outlined below:

$$H = \begin{pmatrix} g(w_1.x_1 + b_1) & \cdots & g(w_M.x_1 + b_M) \\ \vdots & \cdots & \vdots \\ g(w_1.x_N + b_1) & \cdots & g(w_M.x_N + b_M) \end{pmatrix}_{N \times M} \quad .....(13)$$

1.2.2. Computing the target and weight matrices (β and T) using equation (14).

$$\beta = \begin{pmatrix} \beta_1^T \\ \vdots \\ \beta_M^T \end{pmatrix} \quad \text{and} \quad T = \begin{pmatrix} t_1^T \\ \vdots \\ t_N^T \end{pmatrix} \quad ......(14)$$

2. Testing Phase :
2.1. Calculation of Matrix
2.1.1. Computing the matrix of the layer which is hidden (*HO*) by using the equation (13).
2.1.2. Calculating weights of the output by using the equation (15)

$$\hat{\beta} = (H^T H + \lambda I)^{-1} H^T T \quad ......(15)$$

2.1.3. Calculating matrix outcome (*Oj*) by equation (16)

$$O_j = \hat{H}\hat{\beta} \quad ....(16)$$

2.1.4. Getting the class label of testing (*lj*), where *j2 L* and *L* are the number of classes by equation (17).

$$l_j = \arg\max_{j \in L}(O_j) \quad ......(17)$$
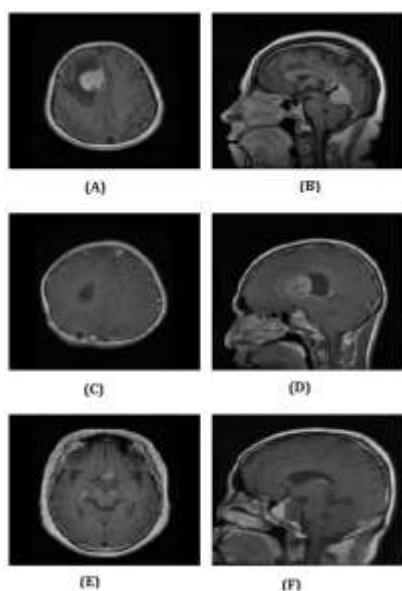
Figure-3: Illustrations of BT images acquire from provided data-set: (A) - (B) Brain tumour with meningioma, (E)-(F) Pituitary Brain Tumour and (C)-(D) Glioma Brain Tumour

B) SETTING of PARAMETERS

The suggested approach necessitates the initialization of multiple parameters. When testing, the grid search technique is employed along with our proficiency in Machine learning and Image Processing to ascertain suitable values for these parameters. The values of parameters utilized in our investigations are presented in Table 1.

Table-1: Parameter Settings

Method	Parameters
RELM	The no. of Hidden Node is $M_{RELM} \in \{1500,1005,1010,1015,..,2000\}$ RELM matrix Search Size =21 The parameter for regulation is expressed as follows: $(\lambda) = \exp(val)$ where $val \in \{-10.2, -10, -9.8, -9.6, ...9.6, 9.8, 10\}$ The function of activation is 'Tan h' $\tanh(x) = \left(\dfrac{2}{1+e^{-2x}} - 1 \right)$
PCA-NGIST	Size of Image =256 X 256=65536 pixels Orientation Number=8 Scales=4 Size of Block = 4 X 4=16 Pixels The no. of Eigen Vectors is $EV \in \{50,150,250,350\}$.

Several of the parameters of the technique were chosen empirically, as was already mentioned. We tested many combinations of eigenvectors and hidden nodes in RELM, for example, and selected the combination of eigenvectors and hidden nodes that produced the best representative features and a high degree of accuracy.

C. EXPERIMENTAL RESULTS

Numerous investigations have been performed using two distinct techniques: the holdout method and the 5-fold approach of cross validation. The dataset got split into two sections using the holdout strategy: a testing data-set having 30% of a data and a training data-set with 70% of a data. With respect to the 5 fold cross checking, the given data-set was apportioned into 5 subsets, 1 for testing and the excess 4 for preparing the same process is repeated 5 times. In the judgement phase, confusion matrices were generated to assess the accuracy of classifying genuine brain tumors and their corresponding types.

	meningioma	glioma	pituitary
meningioma	167	20	12
glioma	28	402	3
pituitary	4	5	278
accuracy	92.17%		

(a)

	meningioma	glioma	pituitary
meningioma	175	18	6
glioma	27	405	2
pituitary	6	4	278
accuracy	93.57%		

(b)

	meningioma	glioma	pituitary
meningioma	177	17	6
glioma	27	406	0
pituitary	5	5	277
accuracy	93.69%		

(c)

	meningioma	glioma	pituitary
meningioma	178	17	7
glioma	19	412	0
pituitary	6	4	277
accuracy	94.25%		

(d)

Figure-4: The outcomes of the confusion matrix are as follows:

(a) Confusion Matrix depicting the outcomes of P C A - N G I S T along with RELM where EVS equals 50.
(b) Displayed Confusion Matrix showcasing the results of P C A - N G I S T along with RELM, with EVS exceeding 150.
(c) Confusion Matrix presentation illustrating the consequences of P C A - N G I S T combined along with RELM, with EVS surpassing 250.
(d) Presented confusion matrix outlining the findings of P C A - N G I S T in conjunction along with RELM, with EVS surpassing 350.

The confusion matrices illustrating the brain tumor classification are depicted in figure:4, employing different eigen vectors (EVs) obtained through PCA using the method holdout. The perfection outcomes derived from the given matrices are computed as mentioned below.

$$((TN+TP))/((TN+FN+TP+FP))$$

$$......(18)$$

In the equation provided, FP represents False-Positive rate and TP represents True-Positive rate. On the other hand, FN represents False-Negative rate and TN represents True-Negative rate. In this equation, we assess the efficacy of the PCA-NGIST with RELM classifier in comparison to other similar methods. Furthermore, it's worth noting that we observed higher classification accuracy when employing the NGIST descriptor as opposed to using GIST.
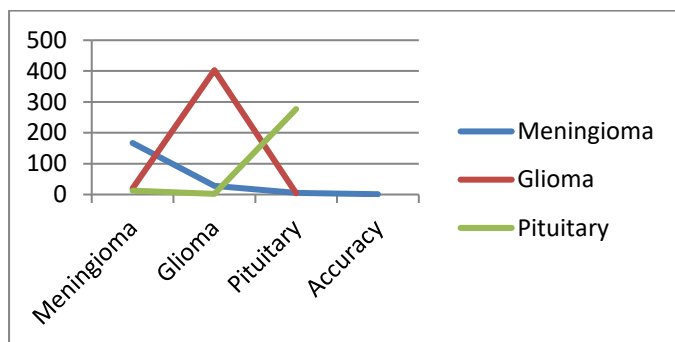
With the help of the 5-folds cross validation procedure, another experiment is conducted. The five distinct testing sets' categorization accuracy ranges from 91.667% to 94.941%, with an average accuracy of 92.6144%. Figure 6 depicts the confusion matrix with the highest degree of classification accuracy.

	meningioma	glioma	pituitary
meningioma	112	16	4
glioma	6	282	0
pituitary	4	3	184
accuracy	95.04%		

Figure-6 Here is an instance of the brain tumor images extracted from the data-set

(a) - (b) meningioma brain tumor, (c) - (d) glioma brain tumor (e) - (f) pituitary brain tumor

Table-2: A comparison is performed to assess the accuracy of brain tumour categorization between the suggested methods and currently established latest approaches.

Reference Paper	Approach	Size of Image	Accuracy
13	RF	256 X 256	90
13	CNN	256 X 256	91.43
12	CNN	64 X 64	84.19
	SVM-RBF	256 X 256	91.51
	DT	256 X 256	81.33
	NB Naïve	256 X 256	66.92
	P C A - N G I S T along with RELM	256 X 256	94.94

To determine how well the proposed method works, table number 2 presents a comparative analysis of classification accuracy between our suggested approach and the utilization of contemporary methodologies. Notably, our recommended strategy demonstrates superior classification accuracy when compared to cutting-edge algorithms such as CNN, SVM-RBF, and NB. This enhanced accuracy can be attributed to the capability of our specialized hybrid feature extraction technique in accurately discerning crucial features for distinguishing various types of brain tumors.

Conclusion:

This paper proposed a three step procedure for precisely categorizing the brain tumors. In the very first step, intensity data from brain images are converted. Then, using the innovative and powerful hybrid approach PCA-NGIST, the most important properties are recovered. In the end,by utilizing the RELM classifiers, brain tumors has been classified. The accuracy of the classification suggested approach is contrasted and assessed by employing a fresh accessible dataset of brain tumor images. There are three different kinds of brain tumours in 3064 brain scans from 233 individuals, which are included in this dataset. The trials include holdout (30% Testing & 70% Training) and cross-validation technique (5-fold). The result of the experimentation show that the P C A – N G I S T feature extraction technique outperforms P C A – G I S T, G I S T, and N G I S T processed towards with respect to the accuracy. Moreover, the outcomes indicated that the mentioned technique in terms of classification accuracy, outperformed current methods. We aim to extend this by comparing and contrasting various machine learning classifiers through the recommended methodology to address a different biological categorization challenge.

REFERENCES:

[1] S. Pereira, A. Pinto, V. Alves, and C. A. Silva, ``Brain tumor segmentation using convolutional neural networks in MRI images,'' IEEE Trans. Med. Imag., vol. 35, no. 5, pp. 1240_1251, May 2016.

[2] E. Dand_l, M. Çak_ro_glu, and Z. Ek^{3}i, ``Computer-aided diagnosis ofmalign and benign brain tumors on MR images,'' in ICT nnova-

tions: Advances in Intelligent Systems and Computing, vol. 311. Cham, Switzerland: Springer, 2015, pp. 157_166.

[3] A. Sehgal, S. Goel, P. Mangipudi, A. Mehra, and D. Tyagi, ``Automatic brain tumor segmentation and extraction in MR images,'' in Proc. Conf. Adv. Signal Process. (CASP), Pune, India, Jun. 2016, pp. 104_107.

[4] C. Sompong and S. Wongthanavasu, ``Brain tumor segmentation using cellular automata-based fuzzy c-means,'' in Proc. 13th Int. Joint Conf. Comput. Sci. Softw. Eng. (JCSSE), Khon Kaen, Thailand, Jul. 2016, pp. 1_6.

[5] G. B. Praveen and A. Agrawal, ``Multi stage classi_cation and segmentation of brain tumor,'' in Proc. 3rd Int. Conf. Comput. Sustain. Global Develop. (INDIACom), New Delhi, India, Mar. 2016, pp. 1628_1632.

[6] S. A. Banday and A. H. Mir, ``Statistical textural feature and deformable model based MR brain tumor segmentation,'' in Proc. 6th Int. Conf. Adv. Comput., Commun. Inform. (ICACCI), Jaipur, India, Sep. 2016, pp. 657_663.

[7] S. Abbasi and F. Tajeripour, ``Detection of brain tumor in 3D MRI images using local binary patterns and histogram orientation gradient,'' Neurocomputing, vol. 219, pp. 526_535, Jan. 2017.

[8] A. Ahmadvand and P. Kabiri, ``Multispectral MRI image segmentation using Markov random _eld model,'' Signal, Image Video Process., vol. 10, pp. 251_258, Feb. 2016.

[9] L. Zhao and K. Jia, ``Deep feature learning with discrimination mechanism for brain tumor segmentation and diagnosis,'' in Proc. Int. Conf. Intell. Inf. Hiding Multimedia Signal Process. (IIH-MSP), Adelaide, SA, Australia, Sep. 2015, pp. 306_309.

[10] X. W. Gao, R. Hui, and Z. Tian, ``Classi_cation of CT brain images based on deep learning networks,'' Comput. Methods Programs Biomed., vol. 138, pp. 49_56, Jan. 2017.

[11] X. W. Gao and R. Hui, ``A deep learning based approach to classi_cation of CT brain images,'' in Proc. SAI Comput. Conf. (SAI), London, U.K., Jul. 2016, pp. 28_31.

[12] N. Abiwinanda, M. Hanif, S. T. Hesaputra, A. Handayani, and T. R. Mengko, ``Brain tumor classi_cation using convolutional neural network,'' in World Congress on Medical Physics and Biomedical Engineering. Singapore: Springer, 2018, pp. 183_189.

[13] J. Paul, ``Deep learning for brain tumor classi_cation,'' M.S. thesis, Dept. Comput. Sci., Vanderbilt Univ., Nashville, TN, USA, May 2016.

[14] A. I³_n, C. Direko§lu, and M. .ah, ``Review of MRI-based brain tumor image segmentation using deep learning methods,'' Procedia Comput. Sci., vol. 102, pp. 317_324, 2016.

[15] G.-B. Huang, Z. Bai, L. L. C. Kasun, and C. M. Vong, ``Local receptive _elds based extreme learning machine,'' IEEE Comput. Intell. Mag., vol. 10, no. 2, pp. 18_29, May 2015.

[16] A. Ari and D. Hanbay, ``Deep learning based brain tumor classi_cation and detection system,'' Turkish J. Elect. Eng. Comput. Sci., vol. 26, no. 5, pp. 2275_2286, 2018.

[17] A. Oliva and A. Torralba, ``Modeling the shape of the scene: A holistic representation of the spatial envelope,'' Int. J. Comput. Vis., vol. 42, no. 3, pp. 145_175, 2001.

[18] A. Gumaei, R. Sammouda, A. Malik S. Al-Salman, and A. Alsanad, ``An improved multispectral palmprint recognition system using autoencoder with regularized extreme learning machine,'' Comput. Intell. Neurosci., vol. 2018, May 2018, Art. no. 8041609.

[19] A. Gumaei, R. Sammouda, A. Malik S. Al-Salman, and A. Alsanad, ``Antispoo _ng cloud-based multi-spectral biometric identi_cation system for enterprise security and privacy-preservation,'' J. Parallel Distrib. Comput., vol. 124, pp. 27_40, Feb. 2019.

[20] T. S. Lee, ``Image representation using 2D Gabor wavelets,'' IEEE Trans. Pattern Anal. Mach. Intell., vol. 18, no. 10, pp. 959_971, Oct. 1996.

[21] J. Yang, D. Zhang, A. F. Frangi, and J.-Y. Yang, ``Two-dimensional PCA: A new approach to appearance-based face representation and recognition,'' IEEE Trans. Pattern Anal. Mach. Intell., vol. 26, no. 1, pp. 131_137, Jan. 2004.

[22] A. Gumaei, R. Sammouda, A. M. Al-Salman, and A. Alsanad, ``An effective palmprint recognition approach for visible and multispectral sensor images,'' Sensors, vol. 18, no. 5, p. 1575, 2018.

[23] G.-B. Huang, X. Ding, and H. Zhou, ``Optimization method based extreme learning machine for classi_cation,'' Neurocomputing, vol. 74, nos. 1_3, pp. 155_163, 2010.

[24] G.-B. Huang, H. Zhou, X. Ding, and R. Zhang, ``Extreme learning machine for regression and multiclass classi_cation,'' IEEE Trans. Syst., Man, Cybern. B. Cybern., vol. 42, no. 2, pp. 513_529, Apr. 2012.

[25] J. Cheng, ``Brain tumor dataset (version 5),'' 2017. doi: 10.6084/m9._gshare.1512427.v5.

[26] J. Cheng et al., ``Enhanced performance of brain tumor classi_cation via tumor region augmentation and partition,'' PLoS One, vol. 10, no. 12, 2015, Art. no. e0144479.